Archaeological Prospection
Archaeol. Prospect. **24**, 59–73 (2017)
Published online 27 November 2016 in Wiley Online Library
(wileyonlinelibrary.com) DOI: 10.1002/arp.1553

On the Use of Fluxgate 3-Axis Magnetometers in Archaeology: Application with a Multi-sensor Device on the Site of Qasr ʻAllam in the Western Desert of Egypt

BRUNO GAVAZZI[1,2*], ROZAN ALKHATIB-ALKONTAR[1], MARC MUNSCHY[1], FRÉDÉRIC COLIN[2,3] AND CATHERINE DUVETTE[2]

[1] *UMR 7516, Institut de Physique du Globe de Strasbourg (IPGS), École et Observatoire des Sciences de la Terre (EOST), Université de Strasbourg/CNRS, Bâtiment Blessig, 1 rue Blessig F-67084 Strasbourg cedex, France*
[2] *UMR 7044, Archéologie et histoire ancienne : Méditerranée – Europe (Archiméde), Maison Interuniversitaire des Sciences de l'Homme – Alsace (MISHA), Université de Strasbourg/CNRS, 5 allée du Général Rouvillois F-67083 Strasbourg cedex, France*
[3] *Institut Français d'Archéologie Orientale (IFAO) 37 rue al-Cheikh Ali Youssef, B.P. 11562 Qasr al-Aïny 11441 Cairo, Egypt*

ABSTRACT Fluxgate 3-axis magnetometers are seldom used on archaeological sites due to their lack of precision. Nonetheless, they offer light weight, low power consumption and the ability of compensation of the magnetization of the prospecting device. This study proposes to use calibration and compensation processes developed for space research and aerial measurement to build a multi-sensor and georeferenced device to assess deep and shallow objects for large-scale archaeological investigations in Qasr 'Allam, in a context of heavy sedimentary coverage and uneven surface. The use of the device on the site in combination with potential field transformations of the signal such as the double reduction to the pole and the vertical derivative reveal a vast irrigation system as well as a large religious facility. A comparison with gradiometric measurements shows a resolution as good at least for shallow sources. The precise positioning allows targeted excavations that validate the geophysical interpretations and offer new archaeological information. These discoveries give enough proof to the local authorities to define the area to be protected from the threatening progression of agricultural fields. Copyright © 2016 John Wiley & Sons, Ltd.

Key words: Magnetometry; 3-axis fluxgate magnetometers; multi-sensors; magnetic compensation; potential field transformations; vertical vector fluxgate

Introduction

Situated in the Western Desert of Egypt, the oasis of Bahariya (Fig. 1) has been inhabited since Prehistory (Svoboda, 2006, 2013). The main phases of the ancient Egyptian civilization can be observed in the area. However, they are not as well documented as in the Nile valley because only a few scholars have studied the Bahariya region. This is mainly due to access difficulties until the construction of the road infrastructure in the mid-twentieth century. A growing number of investigations have taken place since the end of the 1990s. They revealed the archaeological potential of a locally poorly understood period, ranging from the Third Intermediate Period to the Roman times [i.e. from the ninth century BCE to the third century CE (Colin, 2013a, pp. 151–152)]. This article focuses on the site of Qasr 'Allam (Fig. 1), which integrity is threatened by heavy sedimentary processes and the rapid site destruction by recent increases in agricultural development. Magnetometry is used to locate and study the archaeological remains of a historically significant dwelling.

* Correspondence to: Bruno Gavazzi, UMR 7516, Institut de Physique du Globe de Strasbourg (IPGS), École et Observatoire des Sciences de la Terre (EOST), Université de Strasbourg/CNRS, Bâtiment Blessig, 1 rue Blessig, F-67084 Strasbourg cedex, France. E-mail: bgavazzi@unistra.fr

Received 5 February 2016
Revised 10 June 2016
Accepted 5 September 2016

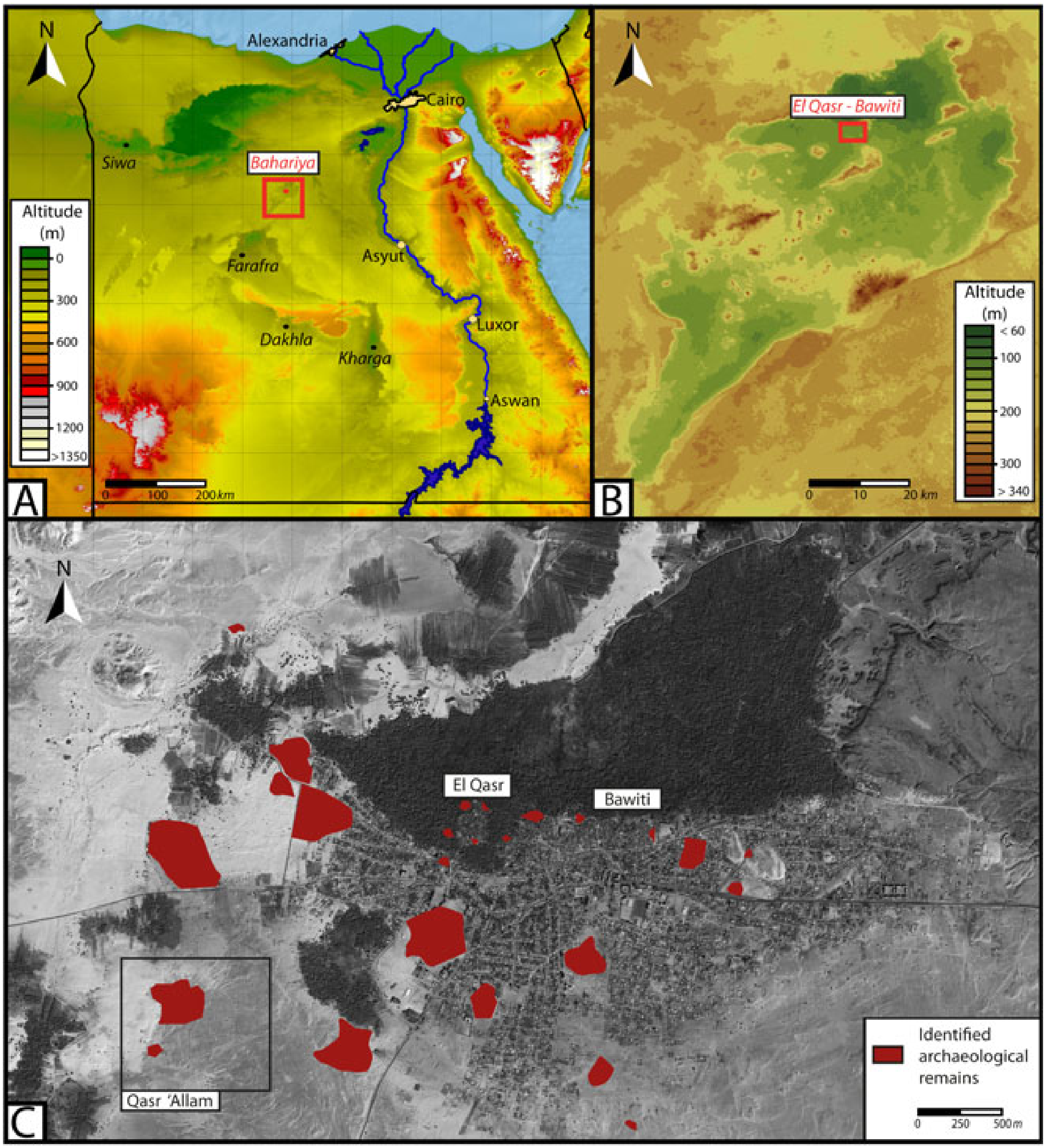

Figure 1. (A) Localization of the oasis of Bahariya on a topographic map of Egypt. (B) Localization of El Qasr-Bawiti on a topographic map of Bahariya. (C) Localization of the site of Qasr ’Allam on a satellite image of El Qasr and Bawiti. Topography from SRTM90 data available at http://srtm.csi.cgiar.org/ (Jarvis *et al*., 2008). Satellite image from the satellites Quickbird taken in 2003 (DigitalGlobe Incorporated, Eurimage SPA licence).

The site of Qasr ’Allam

Before any archaeological study, the site of Qasr ’Allam was known mostly as a rectangular structure emerging from the sand which was interpreted by inhabitants as an Arabic fort (Colin and Labrique, 2003, pp. 169–170). More than 10 years of excavation then revealed facilities buried within sand and mud to be composed of mudbrick buildings of different natures, such as houses, storerooms and workshops (Fig. 2A–2C). These structures were interpreted as part of a wide religious estate, the “Domain of Amun” according to stamped potteries found in the domestic dump sites of the dwellings. Two periods of occupation can be identified from the ninth to the seventh centuries BCE (Colin, 2011, pp. 57–68). A complex network of fossilized irrigation structures have been identified through the traces of wells as well as open and underground channels surrounding the dwelling. Nowadays most of these structures are partially or totally covered with sand and often, only the materials excavated during construction and maintenance are visible on the surface (Fig. 2A, 2D–2F).

DOI: 10.1002/arp

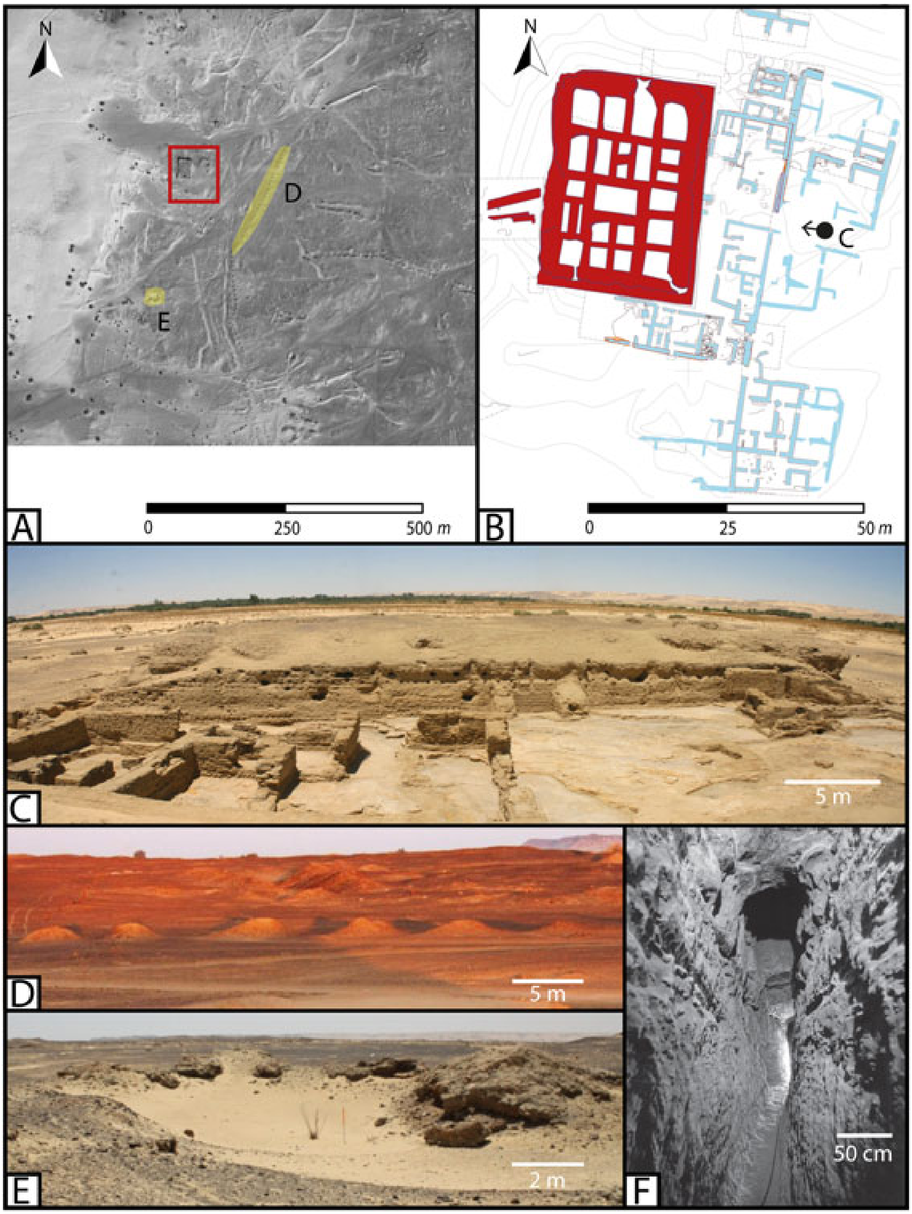

Figure 2. (A) Localization of the excavated dwelling (red) and the irrigation structures of the pictures D and E (yellow) on a satellite image of Qasr 'Allam (DigitalGlobe Incorporated, Eurimage SPA licence). (B) Architectural plan of the excavated dwelling and orientation of the picture C. Blue and red colours corresponds to buildings of a first and second period of occupation. (C) Lateral view of the cellular foundation platform of the second period of occupation. (D) Traces of an underground channel. (E) Traces of a well. (F) Inside of an underground channel similar to the ones of the site and excavated in the oasis of Kharga (Wuttmann *et al*., 1996).

These discoveries might indicate that the site could be a well-preserved example of a complete religious facility with three main components: a religious core, associated domestic buildings and its surrounding agricultural domain, of which most parts are still buried within the ground. The structural organization of the excavated buildings suggests indeed that they were only an annex in the periphery of a much larger and central religious facility (Colin, 2011, pp. 65–66; Colin and Duvette, 2012, pp. 161–162). According to this hypothesis, the direction of the access ramp of a cellular foundation platform (Fig. 2A, 2B), whose typology is well known in the Nile valley (Spencer, 1979a, pp. 116–118; Spencer, 1979b; Traunecker, 1987; Leclère, 2008, pp. 630–636; Malecka-Drozd, 2014), would indicate that the presumed core is located westwards. At present a sand dune a few metres thick covers the area and no archaeological traces are visible on the surface.

However, this hypothesis suffers from two uncertainties: (1) the lack of traces on the surface of the complex core; (2) the lack of information on the spatial and chronological links between the buildings and the irrigation system.

Answers to these problems could be gained from a geophysical image of the sub-surface. The surveying strategy should then take into account strong constraints: the area is highly threatened from the west by agricultural development, increasing every year. Furthermore, the whole dune shows an uneven topography scattered with dried halfa grass and bushes reaching a height up to 0.8 m. Thus, the prospection of the area must be fast and adapted to the roughness of the terrain.

Choice of the geophysical method

In such a context, the most appropriate solution would appear to be the use of magnetic methods. Geomagnetism is a popular and effective method for archaeological purposes (Linford, 2006; Gaffney, 2008). The main advantages are: (1) the anthropic traces usually show a strong contrast of magnetization with their surroundings; (2) the rapidity of measurement and light weight of the sensors allow mapping of large surfaces with a high density of data. In addition, Tomasz Herbich (2011) has conducted a first prospection using vector gradiometer (Geoscan FM256) between the sand dune and the platform in 2006 and 2010. It revealed irrigation structures as well as walls and foundation trenches (Colin, 2006, 2010; Herbich, 2011), thus giving evidence of a contrast of magnetization strong enough to identify the archaeological remains. However, the study of Herbich (2011) also revealed some limitations over the sand dune: the topography and vegetation make the implementation of a grid and the measurements less than 0.8 m above the ground highly difficult without an intense preparation of the field. Moreover, one of the properties of the vertical gradient is to enhance short wavelength and to smooth out large wavelength variations of the magnetic field. This makes gradiometers extremely sensitive to shallow objects but of limited capability to identify deeper sources or lower magnetic contrasts as is the case for Qasr ’Allam (Blakely, 1995, pp. 324–326; Fagaly, 2001, pp. 327–328). This article proposes to overcome these limitations by adapting the measurement of the total magnetic field with 3-axis vector fluxgate magnetometers, usually used in space research or mining exploration (Nabighian *et al.*, 2005), and more recently for the detection of unexploded ordnances (Munschy *et al.*, 2007), to archaeological surveys.

Method

Device

The core of the developed method lies in the measurement of the intensity of the magnetic field with fluxgate magnetometers. Such magnetometers (Fig. 3A) have the advantage of being light (80 g) and consuming

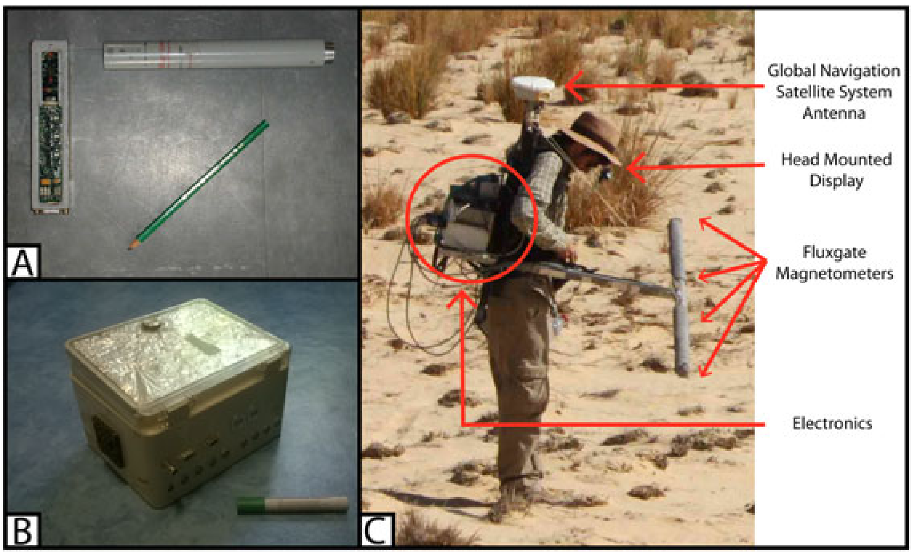

Figure 3. (A) A 3-axis fluxgate magnetometer (Bartington Inc., Mag-03 MC). (B) Custom electronics with eight magnetometer inputs developed by Institut de Physique du Globe de Strasbourg (IPGS). (C) Multi-sensor device developed by IPGS.

DOI: 10.1002/arp

low energy (<1 W). Their three orthogonal sensors allow the measurement of the three components of the magnetic field at a rate greater than 1000 Hz (Primdahl, 1979), from which the total magnetic field can easily be calculated. The device developed for this study (Fig. 3C) is built around in-house developed electronics (Fig. 3B). It powers the rest of the instrument, digitizes and stores the data of one to eight magnetometers as well as one to two global navigation satellite system (GNSS) antennas. The electronics are mounted on a backpack and four magnetometers are placed 0.5 m apart from each other in front of the operator, 1 m above the ground. A GNSS antenna is placed at the top of the backpack for the navigation. Both navigation and magnetic data are displayed in real time through a head mounted display (HMD). The device weighs less than 15 kg and can be operated by a single person who follows parallel survey lines set every 2 m and displayed in the HMD. Thus, georeferenced magnetic profiles are acquired every 0.5 m centred on each survey line without any preparation on the field. In Qasr ʼAllam, 5000 m^2 to 12000 m^2 of magnetic data were acquired per hour of measurement.

Calibration and compensation

A major disadvantage of the fluxgate magnetometer is that it is a relative device. This means that the instrument requires a precise calibration before each session of measurements to correct errors of sensitivity, offset and angle. This problem is well known and various techniques of calibration have been developed. In this study the calibration is done using a process developed initially for space research (Olsen *et al.*, 2003). It consists in the rotation of the magnetometers (or the whole device) in all direction around a fixed point where the magnetic field can be considered steady. The registered variations of the magnetic field are therefore only due to the different kinds of errors which can then be minimized using a least squares method. The advantage of the process is that it also compensates for the remnant and induced magnetization of the device itself (Munschy *et al.*, 2007). This makes the fluxgate the only magnetometer capable of such compensation, allowing compact multi-sensor devices as well as motorized measurements. A typical result of the effect of the calibration and compensation process on a magnetometer is shown in Fig. 4, where computed parameters reduce the variations of measurements at a fixed point from around 200 nT to 0.3 nT.

Time-dependant variations

Another issue with the measurement of the total magnetic field is the correction of the time-dependant variations which may be caused by extra-terrestrial sources or anthropic activities. Additionally, fluxgate magnetometers are not absolute and subject to drift with the change of temperature (0.1 to 0.5 nT/°C according to the manufacturer). In an environment affected by homogeneous but not linear temporal variations, as is often the case in urban areas, corrections can be made by using a magnetometer installed at a fixed point (base station) during the measurements, thus recording only the time dependant part of the signal. Such solution was not possible in Qasr ʼAllam due to legal and logistical difficulties to have a base station on the site at the time of the study. However, during the surveying hours (6:00 to 10:00 a.m.), time-dependant variations are linear and can therefore be easily corrected. They are the result of a combination of effects from a temperature drift as well as from far external sources of which the linear variation is confirmed by using geomagnetic records of one of the nearest INTERMAGNET observatory (Tamanrasset).

Data processing

The measurement provides the three calibrated components of the total magnetic field, from which the total magnetic intensity is calculated. In archaeology, the prime interest is to measure/illustrate subtle spatial variations of the magnetic field. This is achieved by observing the anomalies of the total magnetic field's intensity. The anomaly is defined as the difference between the intensity of the measured magnetic field and the regional field (Blakely, 1995, pp. 178–180). The latest is computed using the International Geomagnetic Reference Field (IGRF) (Finlay *et al.*, 2010). The anomaly of the intensity of the total magnetic field can then be displayed either as profiles or as maps after a gridding computerized operation (D'Errico, 2005). The node distance of the grid is usually set as half of the distance between each magnetometer, i.e. 0.25 m in this study. After this procedure, the residual errors can lead to the appearance of a levelling effect between profiles (Fedi and Florio, 2003). To solve this problem, the differences at the crossing points between the values on magnetic profiles (in-lines) and traverses (tie-lines) are measured. Then, a constant to apply to each profile is calculated by a linear inversion to minimize the differences at the crossing points.

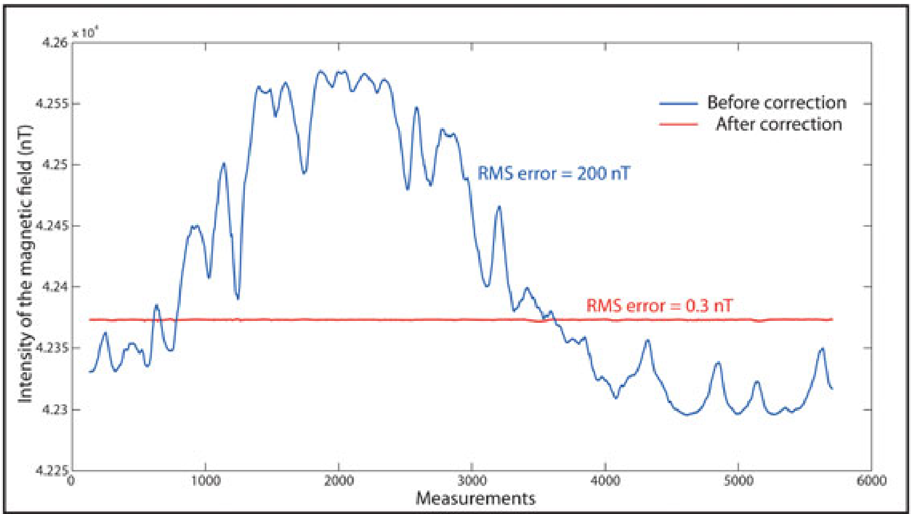

	Sensitivity (coefficient)	Offset (nT)	Angle (°)
Sensor X	0.999698 (+/- 0.000002)	12.0 (+/- 0.1)	0.062493 (+/- 0.000134)
Sensor Y	1.000807 (+/- 0.000010)	- 30.3 (+/- 0.4)	- 0.055513 (+/- 0.000087)
Sensor Z	1.001029 (+/- 0.000003)	- 16.6 (+/- 0.1)	0.337479 (+/- 0.000286)

Figure 4. Intensity of the magnetic field measured by one magnetometer during the calibration and compensation process of the device before (blue) and after (red) corrections. Computed error parameters are given in the lower part of the figure.

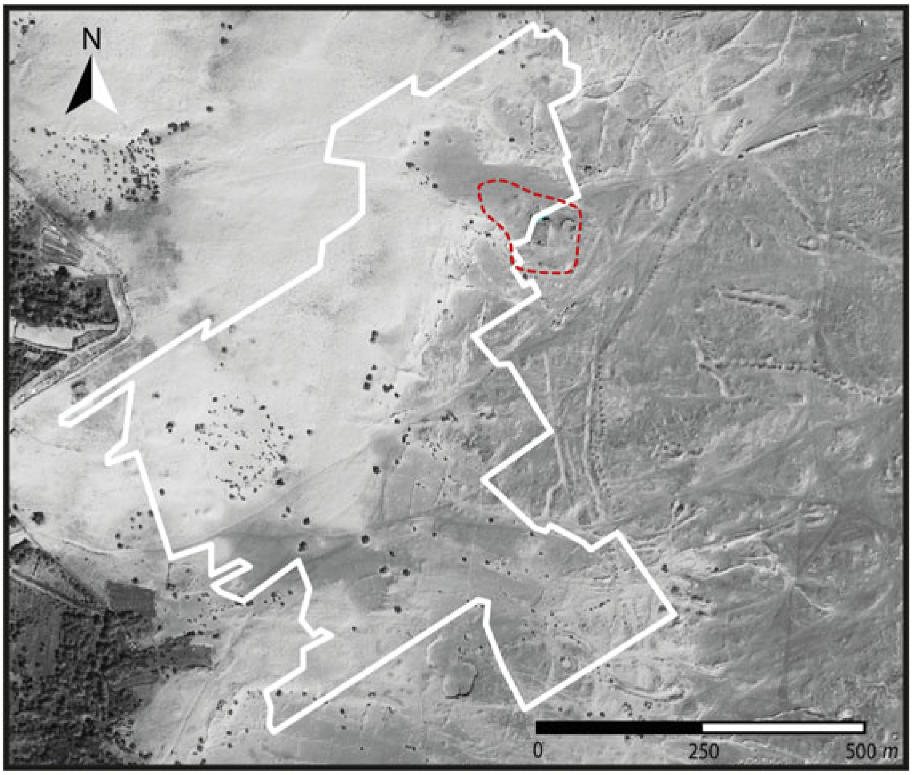

Figure 5. Satellite image of Qasr ’Allam (DigitalGlobe Incorporated, Eurimage SPA licence). The area of the geomagnetic prospection is delimited by the white line. The area of the excavated dwelling is delimited by the red line.

DOI: 10.1002/arp

Results

The data acquisition over the Qasr 'Allam site took place in April and May 2012. Through 200 km of survey lines, more than 800 km of georeferenced magnetic profiles were recorded over an area about 340,000 m^2 (Fig. 5).

Maps of magnetic anomalies

Usually, magnetic anomalies are represented using maps with a linear colour scale. Those consist in attributing a colour or grey tone to each node of the grid according to its value using a linear scale, as shown in Fig. 6. Unfortunately, such a representation is often not sufficient to show accurately all the anomalies of a site, as they can range from a few to hundreds of nano-Tesla. A common solution to this problem is to display multiple maps with different scales to understand the anomalies from the largest to the smallest. Such a process might be time consuming and is not the most practical, as several maps have to be observed at the same time. To overcome this problem, we introduce another approach, the equi-populated mapping. An equi-populated map consists in attributing a shade (or colour) to each node using a non-linear scale in such a way that all the shades are evenly distributed on the map. Thus, both small and strong magnetic anomalies can be represented on a unique map, as shown in Fig. 7.

From both representations (Figs. 6, 7), different kind of anomalies can be observed on the site. Depending on their wavelength and shape, they can be ranked as follows.

- Dipolar anomalies: the strongest one in the west is due to a metallic pole; the others are due to pieces of metal which are scattered everywhere on the site, showing no particular distribution.
- Short wavelength lineation (about 1 m and less): they are the most common anomalies and can be sorted in different subgroups. In the southern part, a high concentration of curved lines following roughly

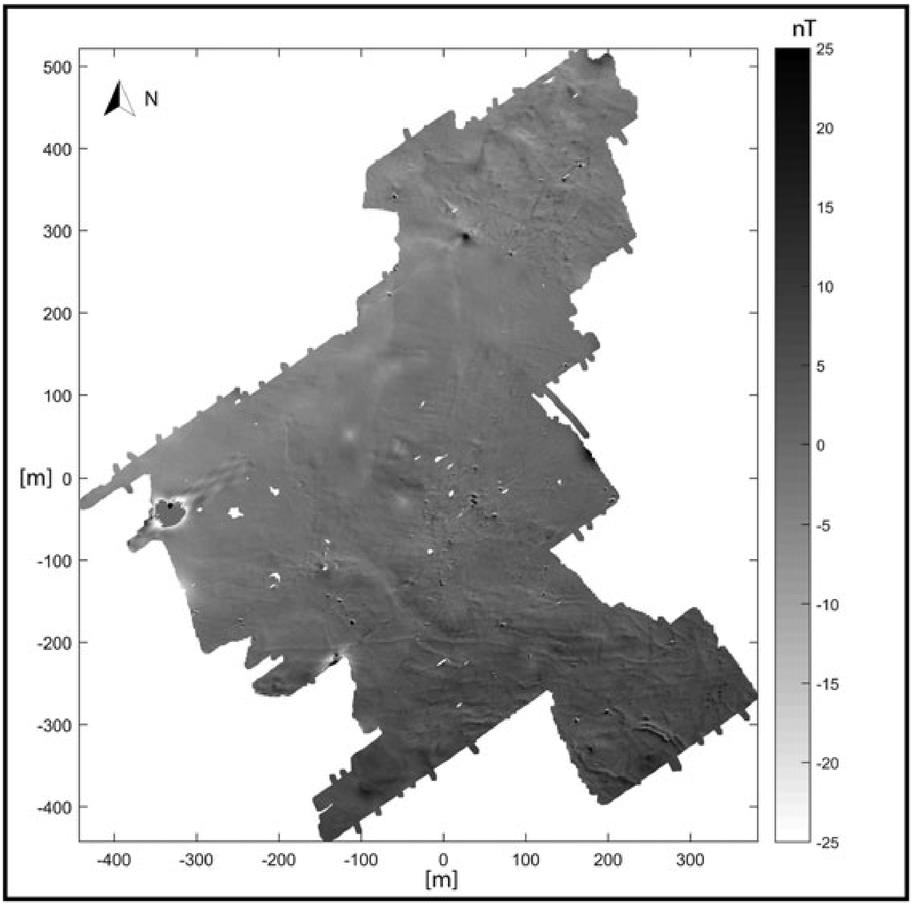

Figure 6. Map of the magnetic anomaly represented with a linear greyscale bar ranging from −25 to 25 nT.

DOI: 10.1002/arp

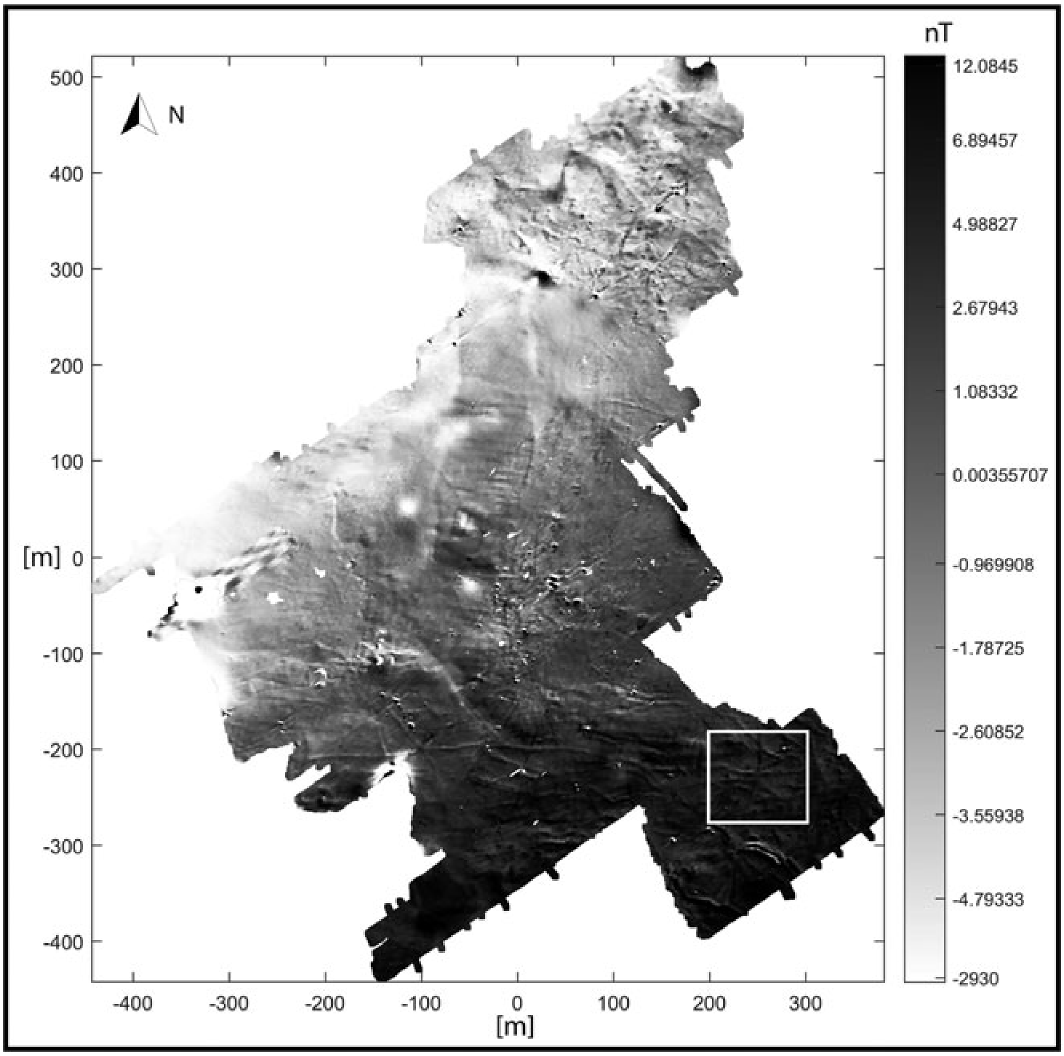

Figure 7. Map of magnetic anomalies represented with an equi-populated greyscale bar. The area delimited by the white line corresponds to the area displayed in Fig. 8.

north–south and east–west orientations is present. A similar pattern can be seen in the northern part, though in much smaller quantities. In the central part, the lines are straighter and follow an orientation similar to the one of the large wavelength lineation surrounding them.

- Large wavelength lineation (about 10 m): they approximatively draw two rectangles of 150 m × 100 m and 125 m × 100 m in the central part of the map. Their orientation is of a few degrees east.
- North–south gradient: the magnetic anomaly field decreases by about 20 nT from north to south. This gradient cannot be explained by the regional magnetic field as the IGRF gives an increase of 3.8 nT from north to south. Thus, it is likely that such a gradient is due to a deep local variation of the underlying geology.

These anomalies reveal the presence of different kinds of magnetic heterogeneities within the ground. Unfortunately, the shape, amplitude and position of an anomaly (as well as the gradient) depend on multiple factors such as the shape, the orientation, the position and magnetization of the source as well as the orientation of the regional magnetic field. To decipher these anomalies, interpretation tools can be found in potential field theory.

Potential field transformations

In any kind of magnetometry, the horizontal position of the sources is situated somewhere in-between the positive and negative extrema of a skewed anomaly. When the wavelength is shorter than the size of the object, as it is often the case for very shallow objects, this is not a problem. Otherwise, as it is often the case in this study, the error can reach up to a few metres, which is not acceptable to locate properly archaeological trenches. Fortunately, the position of the remains can be obtained by using a potential field transformation known as the double reduction to the pole (DRP). The DRP consists in the calculation of the signal when both the magnetization and regional field are set vertical. Thus the anomalies become symmetrical with their maxima above their sources (Baranov, 1957). In the spectral domain, the operation is easily done by multiplying the spectrum of the anomaly by

$$\left[\frac{i\sqrt{u^2+v^2}}{au+bv+ic\sqrt{u^2+v^2}}\right]\left[\frac{i\sqrt{u^2+v^2}}{a'u+b'v+ic'\sqrt{u^2+v^2}}\right] \quad (1)$$

where u and v are the wavelengths associated with x and y directions, $i^2=-1$, (a,b,c) the components of the unit vector in the direction of the regional magnetic field, and (a',b',c') the components of the unit vector in the direction of the magnetization (Bhattacharyya, 1965). The direction of the regional field is given by the IGRF while the direction of magnetization is either set as the same as the regional field when the ratio remnant/induced magnetization is near zero or obtained through successive iterations until the signal become symmetrical. In Qasr ’Allam, as the buildings are made of mudbricks, the orientation of magnetization was set equal to that of the regional field. In Fig. 8, the anomalies become symmetrical, confirming this induced-only magnetization hypothesis. It must be noted that a simple reduction to the pole (only one vector set vertical) does not give the position of the source (Fig. 8). The calculated DRP map gives therefore the position of sources visible or not on the surface (Fig. 9). The archaeological interpretation remains difficult due to the presence of a very large wavelength anomaly most probably due to geology. An easy way to enhance the shortest wavelength while smoothing the largest ones is the use of the vertical derivative. The operation is straightforward in the spectral domain and corresponds to the multiplication of the spectrum of the map by

$$\left(\sqrt{u^2+v^2}\right)^n, \quad (2)$$

where u and v are the wavelengths associated with x and y directions and n is the order of derivation. Fig. 10 corresponds to the map obtained after computing the vertical gradient of the DRP. It can be observed that the different lines are indeed enhanced and, most importantly, new lineations appear, especially in the central area.

Comparison with gradiometry

To assess the quality of the data for archaeological interpretation compared to gradiometry, the area surveyed by Herbich (2011) with a fluxgate gradiometer (Geoscan FM256) was also covered with the device developed in this study. The comparison of the results (Fig. 11) shows that the proposed method reveals at least as much information as a vector gradiometer, even though the magnetometers are more distant from the ground (1 m). The vertical derivative map (Fig. 11A) appears more blurred than the gradiometric map (Fig. 11B) because it corresponds to a more distant acquisition from the sources.

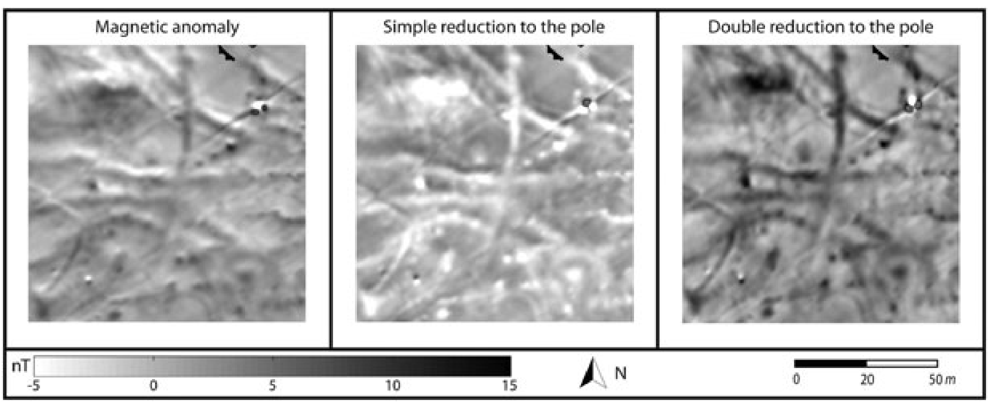

Figure 8. From left to right, map of the magnetic anomaly for a sampled zone of Qasr ’Allam (Fig. 7), reduction to the pole of the regional magnetic field and double reduction to the pole. The IGRF-11 was used to obtain the direction to the regional magnetic field and the magnetization direction is set equal to the IGRF direction.

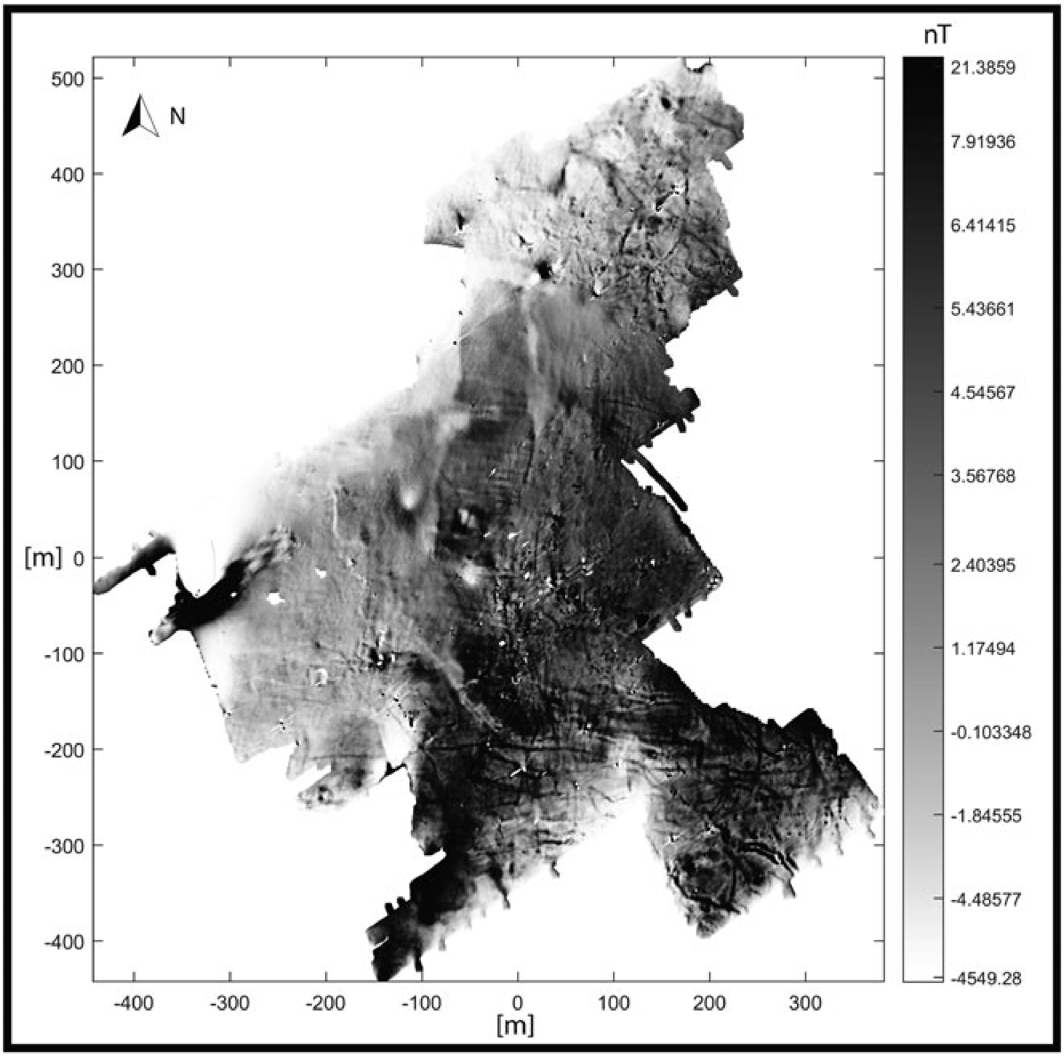

Figure 9. Map of the magnetic anomaly after double reduction to the pole represented with an equi-populated greyscale bar.

Discussion

Interpretation of magnetic anomalies

The different maps give important information on the sources of the magnetic anomalies. The different linear anomalies can be interpreted as highly probable archaeological remains and are divided into three categories: long wavelengths, straight and non-straight short wavelengths. The non-straight linear elements with short wavelengths follow the same rough orientation pattern and shape as the irrigation structures visible on the ground surface. Some of them directly follow the traces of the irrigation structures observed on the ground surface. They are also mostly connected to an area of visible wells in the south-eastern part of the site (Figs. 2, 5). This strongly suggests that those anomalies can be interpreted as irrigation structures, present not only under the sand dune, but also within the harder ground in the whole area (Fig. 12). A targeted excavation of such a structure within the sand dune (Fig. 12, area 15) confirmed open irrigation channels under 1.2 m of sediments (Colin and Duvette, 2012, pp. 163–164). The filling sediments of one segment contained artefacts (potteries, terracotta figurines) of a well-attested type, according to the local typology of the eighth or the seventh century BCE (Colin and Duvette, 2012, p. 164). This information validates the hypothesis that at least one part of the irrigation network was contemporary to the religious complex and that these farming devices most probably belonged to the religious estate.

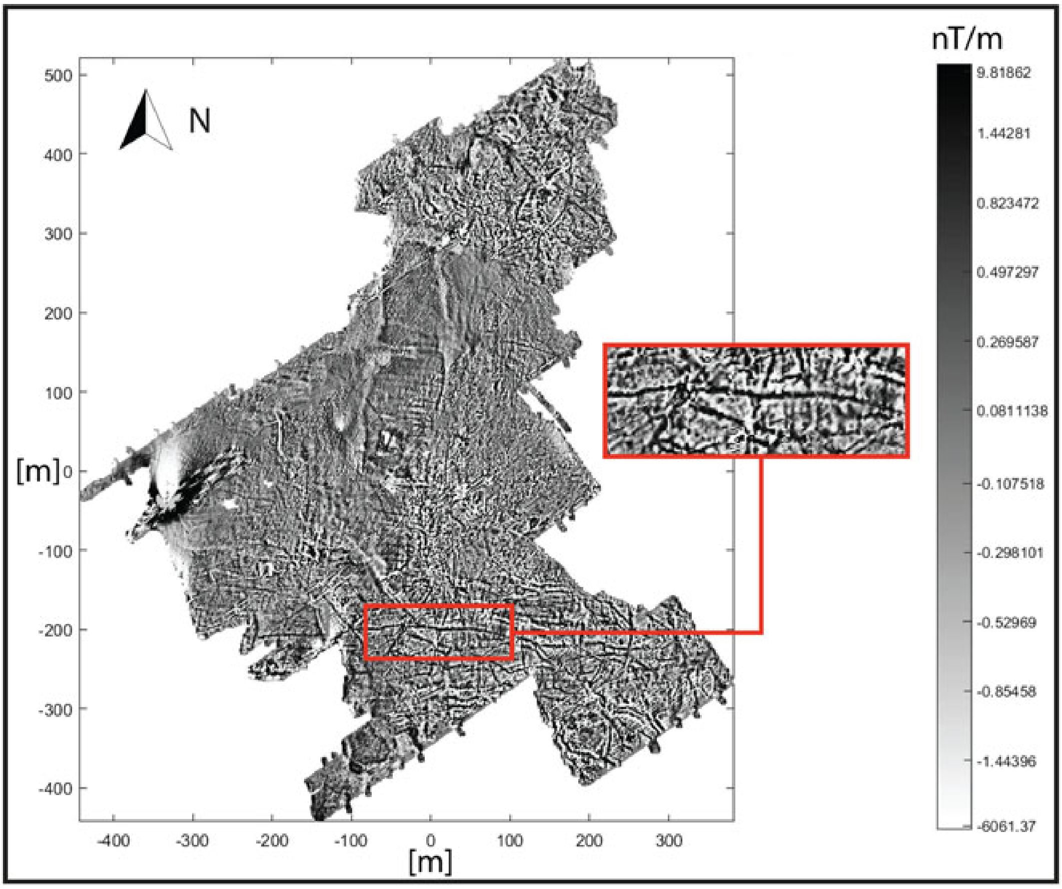

Figure 10. Map of the vertical derivative of the magnetic anomaly after double reduction to the pole represented with an equi-populated greyscale bar. The enlargement corresponds to the area delimited in red.

The two other types of linear anomalies can be interpreted differently. They are situated in front of the access ramp of the platform, where the rest of a religious facility can be expected. They show angular shapes, and display an orientation similar to the one of the already excavated constructions. It can therefore be stated that they most likely correspond to ancient buildings, thus enlarging the surface of the whole facility from 40,000 m^2 to 150,000 m^2 (Fig. 12). The variability of wavelengths can be explained as different depths of sources, either due to the variability of the post-abandonment sedimentary deposits, to different sizes of structures or to successive archaeological periods. This is verified by two targeted excavations which started in 2013 and 2014 and are still in progress (Fig. 12, areas 16 and 17). They revealed the presence of religious buildings corresponding to the magnetic anomalies at different depths from 0.15 to 2.4 m (Fig. 12, area 16 and 17, respectively), which are related to different occupations from at least the eighth or the seventh century BCE to the second century CE and are affected by environmental change (Colin, 2013b; Colin *et al.*, 2014). The stratigraphy of the tested areas revealed that the sedimentary processes followed two successive patterns. The ruins of the last occupation period (Roman) are mainly covered by aeolian sand in an arid context, but the remains of the former periods (from Third Intermediate Period until Late Period or later) are filled with alluvial earthen sediments, in a seemingly more humid context.

The 3-axis fluxgate magnetometer total magnetic field approach

In addition to the interpretation results, the study reveals the potential of the use of the 3-axis fluxgate magnetometers for large-scale archaeological surveys. The light weight of the magnetometers and their compensation ability allow the construction of a compact multi-sensors device which can be operated by a single operator. At least four simultaneous

DOI: 10.1002/arp

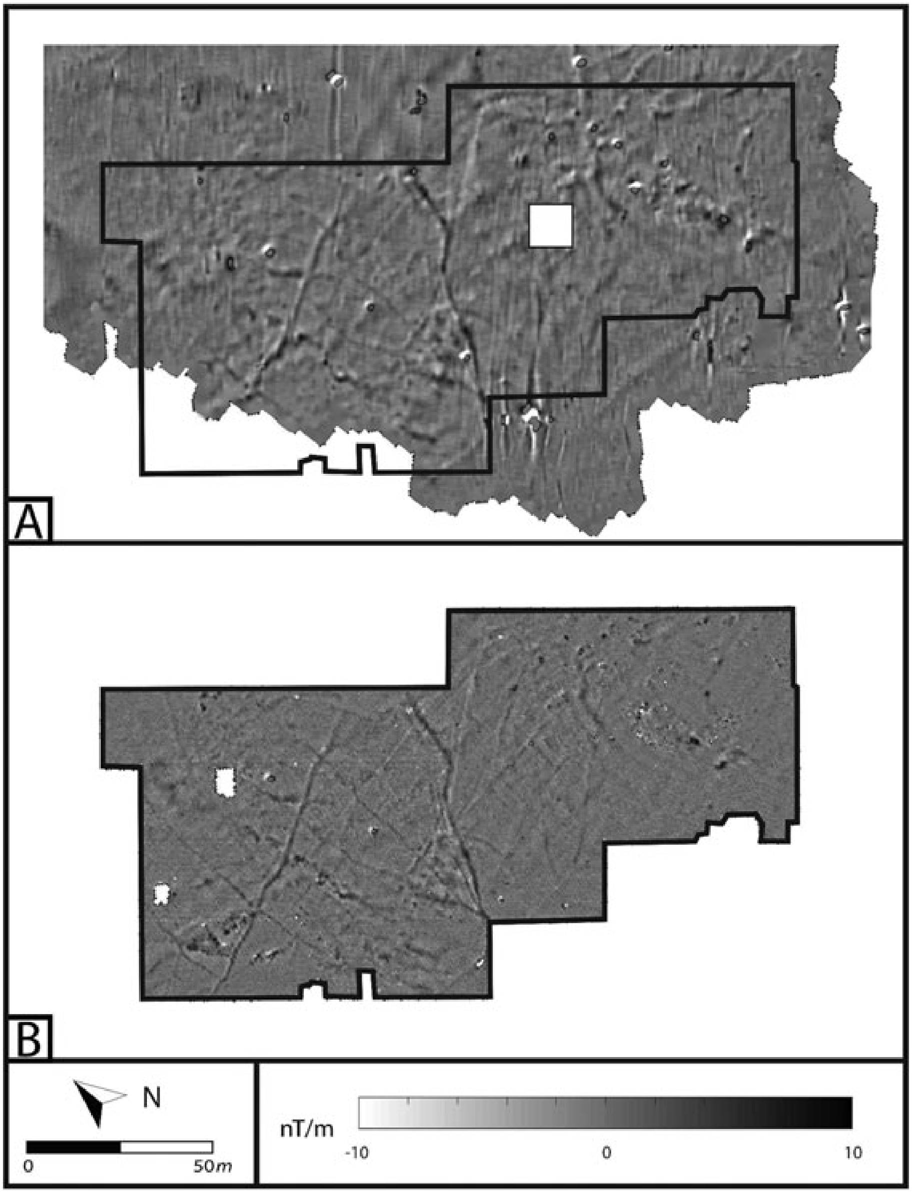

Figure 11. (A) Map of the vertical gradient computed from the data measured with the device developed by Institut de Physique de Globe de Strasbourg (using a vertical derivative). (B) Map of the vertical gradient computed from the data measured by teams directed by Tomasz Herbich with a vector gradiometer Geoscan FM256 during previous surveys (Herbich, 2011).

georeferenced magnetic data without any preliminary preparation of the site can be acquired. The position of the magnetometers 1 m above the ground surface allow areas with more vegetation or a more uneven topography to be covered than with a gradiometer device. Using vertical gradiometry, the lower probe is usually situated 0.2–0.3 m above the ground surface. Thus, the proposed approach proved to be capable to survey 5000 to 12,000 m^2 per hour with a 0.5 m spacing and reveal at least as much information on archaeological remains as a gradiometer through the use of the vertical derivative of the signal (Fig. 11). The application of the DRP gives theoretically the exact horizontal position of the sources, unlike a single reduction which leads to a residual skewness. If the difference or even the use of a reduction can be negligible for very shallow sources, it is not the case with deeper sources, as shown in Fig. 8 and the comparison between Figs. 7 and 9.

DOI: 10.1002/arp

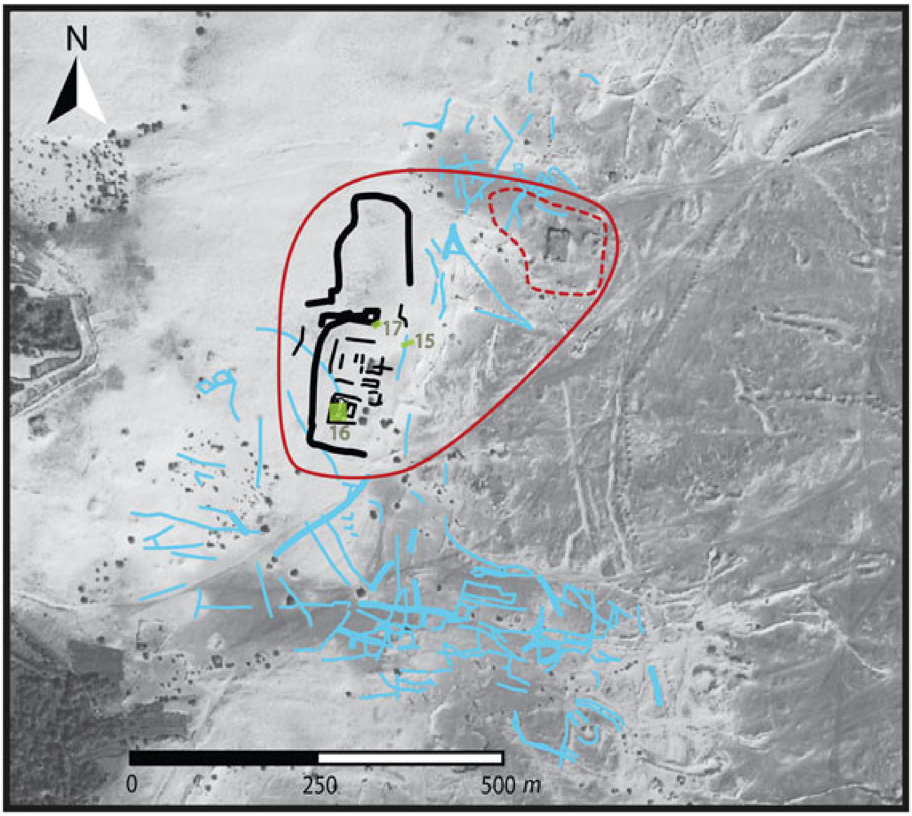

Figure 12. Interpretative map of the archaeological remains from the geomagnetic prospection. The hydraulic structures are represented in blue, the buildings in black. The dotted and plain red lines mark the minimal limits of the dwelling known before and after the study. The areas highlighted in green correspond to three excavations numbered 15, 16 and 17.

Conclusion

The study both validates the application of an innovative approach to magnetic prospections in archaeology and reveals important information on the site of Qasr ʼAllam.

The use of the 3-axis fluxgate magnetometers and associated potential field transformations proved to be efficient to reveal information on both deep and shallow archaeological sources at a large and rapid scale. The results obtained in Qasr ʼAllam offer two prospects for further development: (1) doubling the speed of acquisition by doubling the number of magnetometers; (2) using the compensation ability to develop a smaller device which allows a few centimetres spacing between sensors for high precision small-scale surveys.

In Qasr ʼAllam, the geophysical survey strengthens the hypothesis of the archaeologists. It locates remains of large-scale buildings positioned in the expected area, whose general plan and direction are consistent with the hypothesis of a religious complex which combines a main religious centre (totally covered by sediments) with economic and domestic facilities (of which parts were previously excavated). The accurate positioning of probable archaeological structures has allowed the setting up of targeted excavations that has led to important results. It can be shown that parts of the irrigation network were already being used from the eighth or seventh century BCE in the vicinity of the buildings. That the site was used for religious purposes to at least the second century CE and was impacted by a rapid environmental change from humid to arid in the latest periods of occupation. Without the results provided by the magnetic mapping, the thickness of the sedimentary deposits would have discouraged any attempt to explore the underground by means of the classical archaeological digging methods. A next step would be to investigate further the supposed religious centre and the associated environmental change to find further chronological and functional data. According to its size and the thickness of sediment, the study would need the

DOI: 10.1002/arp

combination of archaeological excavations and a more detailed geophysical method. In consequence, these conclusions encouraged the Egyptian Supreme Council of Antiquities (SCA) to define an area to be protected in 2014 to avoid the destruction of remains by the fast progression of agricultural fields.

Acknowledgements

Some of the results presented in this article rely on the data collected at Tamanrasset observatory. The authors thank the Centre de Recherche en Astronomie, Astrophysique et Geophysique as well as Institut de Pysique du Globe de Paris, for supporting its operation and INTERMAGNET for promoting high standards of magnetic observatory practice (www.intermagnet.org). The authors are grateful to Tomasz Herbich and his team for sharing their data from which the gradiometry map presented in this article was computed. The authors would like to thank the Initiatives d'Excellence (IdEx, Programme Investissements d'Avenir) of the University of Strasbourg for their financial support as well as Laurent Ameglio, Daniel Sauter, Nicolas Florsch, Chris Gaffney and the two anonymous reviewers for their advice and constructive comments.

References

Baranov V. 1957. A new method for interpretation of aeromagnetic maps: pseudo-gravimetric anomalies. *Geophysics* **22**: 359–383. DOI:10.1190/1.1438369.

Bhattacharyya BK. 1965. Two-dimensional harmonic analysis as a tool for magnetic interpretation. *Geophysics* **30**: 829–857. DOI:10.1190/1.1439658.

Blakely RJ. 1995. Potential Theory in Gravity and Magnetic Applications. Cambridge University Press: Cambridge.

Colin F. 2006. Bahariya. In *Travaux de l'Institut Français d'Archéologie Orientale en 2005–2006*, Pantalacci L, Denoix S (eds). *Bulletin de l'Institut Français d'Archéologie Orientale* **106**: 404–409.

Colin F. 2010. Bahariya. In *Travaux de l'Institut Français d'Archéologie Orientale en 2009-2010*, Midant-Reynes B, Denoix S (eds). *Bulletin de l'Institut Français d'Archéologie Orientale* **110**: 326–331.

Colin F. 2011. Le « Domaine d'Amon » à Bahariya de la XVIII[e] à la XXVI[e] dynastie: l'apport des fouilles de Qasr 'Allam. In *La XXVI[e] Dynastie Continuités et Ruptures. Actes Du Colloque International Organisé Les 26 et 27 Novembre 2004 à l'Université Charles-de-Gaulle – Lille 3. Promenade Saïte Avec Jean Yoyotte*, Devauchelle D. (ed.). Paris; 47–84.

Colin F. 2013a. Les gisements archéologiques de Psôbthis au début du XXI[e] siècle: Diagnostic sur un paysage menacé et nouvelles orientations de recherche. In Bahriya Oasis: Recent Research into the Past of an Egyptian Oasis, Dospěl M, Suková L (eds). Charles University: Prague; 151–184.

Colin F. 2013b. Bahariya. Pratiques funéraires et lieux de culte. In *Rapport d'activité 2012–2013*, Midant-Reynes B (ed.). *Supplément au Bulletin de l'Institut Français d'Archéologie Orientale* **113**: 246–251.

Colin F, Duvette C. 2012. Bahariya. Pratiques funéraires et lieux de culte. In *Rapport d'activité 2011–2012*, Midant-Reynes B (ed.). *Supplément au Bulletin de l'Institut Français d'Archéologie Orientale* **112**: 159–165.

Colin F, Duvette C, Gavazzi B, Munschy M, Schuster M, Schwarz D. 2014. Bahariya. Pratiques funéraires et lieux de culte. In *Rapport d'activité 2013–2014*, Midant-Reynes B (ed.). *Supplément au Bulletin de l'Institut Français d'Archéologie Orientale* **114**: 195–201.

Colin F, Labrique F. 2003. Recherches de terrain en Égypte. *Chronique. Dialogues d'histoire ancienne* **29**(2): 165–185. DOI:10.3406/dha.2003.1569.

D'Errico J. 2005. Surface fitting using gridfit. MATLAB Central File Exchange. http://www.mathworks.com/matlabcentral/fileexchange/loadFile.do?objectId=8998

Fagaly RL. 2001. Supercoducting Quantum Interference Devices (SQUIDs). In Magnetic Sensors and Magnetometers, Ripka P (ed). Artech House: Boston, MA; 305–347.

Fedi M, Florio G. 2003. Decorrugation and removal of directional trends of magnetic fields by the wavelet transform: application to archaeological areas. *Geophysical Prospecting* **51**: 261–272. DOI:10.1046/j.1365-2478.2003.00373.x.

Finlay CC, Maus S, Bondar TN, *et al.* 2010. International Geomagnetic Reference Field: the eleventh generation. *Geophysical Journal International* **183**: 1216–1230. DOI:10.1111/j.1365-246X.2010.04804.x.

Gaffney C. 2008. Detecting trends in the prediction of the buried past: A review of geophysical techniques in archaeology. *Archaeometry* **50**: 313–336. DOI:10.1111/j.1475-4754.2008.00388.x.

Herbich T. 2011. Geophysical surveying in Egypt: Periodic report for 2009–2011. In *Archaeological Prospection. Ninth International Conference on Archaeological Prospection*, Drahor MG, Berge MA (eds). Izmir September 19–24; 234–239.

Jarvis A, Reuter HI, Nelson A, Guevara E. 2008. Hole-filled seamless SRTM data V4. International Centre for Tropical Agriculture (CIAT). http://srtm.csi.cgiar.org

Leclère F. 2008. *Les villes de Basse Égypte au Ier millénaire av. J.-C. Analyse archéologique et historique de la topographie urbaine*, Bibliothèque d'étude 144/2. Cairo: IFAO.

Linford N. 2006. The application of geophysical methods to archaeological prospection. *Reports on Progress in Physics* **69**: 2205–2257. DOI:10.1088/0034-4885/69/7/R04.

Malecka-Drozd N. 2014. The emergence and development of architecture on the casemate foundation platforms in the Nile Delta. *Recherches Archéologiques Nouvelle Série* **4**: 69–96.

Munschy M, Boulanger D, Ulrich P, Bouiflane M. 2007. Magnetic mapping for the detection and characterization of UXO: Use of multi-sensor fluxgate 3-axis magnetometers and methods of interpretation. *Journal of Applied Geophysics* **61**: 168–183. DOI:10.1016/j.jappgeo.2006.06.004.

Nabighian MN, Grauch VJS, Hansen RO, *et al.* 2005. 75th Anniversary: The historical development of the magnetic method in exploration. *Geophysics* **70**: 33–61. DOI:10.1190/1.2133784.

Olsen N, Tøffner-Clausen L, Sabaka TJ, *et al.* 2003. Calibration of the Ørsted vector magnetometer. *Earth, Planets, and Space* **55**: 11–18. DOI:10.1186/BF03352458.

Primdahl F. 1979. The fluxgate magnetometer. *Journal of Physics E: Scientific Instruments* **12**: 241–253. DOI:10.1088/0022-3735/12/4/001.

Spencer AJ. 1979a. Brick Architecture in Ancient Egypt. Warminster: Aris & Philips.

Spencer AJ. 1979b. The brick foundations of Late Period peripteral temples and their mythological origin. In Glimpses of Ancient Egypt. Studies in Honour of H. W. Fairman, Ruffle J, Gaballa G, Kitchen K (eds). Aris & Philips: Warminster; 132–137.

Svoboda JA. 2006. Prehistory of the southern Bahariya Oasis, Western Desert, Egypt. An outline. *Archaeology, Ethnology and Anthropology of Eurasia* **28**: 18–30. DOI:10.1134/s1563011006040037.

Svoboda JA. 2013. Prehistory of the Southern Bahariya: A case study in northeast African settlement archaeology. In Bahriya Oasis. Recent Research into the Past of an Egyptian Oasis, Dospěl M, Suková L (eds). Charles University: Prague; 35–62.

Traunecker M. 1987. Les 'temples hauts' de Basse époque: un aspect du fonctionnement économique des temples. *Revue d'égyptologie* **38**: 147–162. DOI:10.2143/RE.38.0.2011639.

Wuttmann M, Bousquet B, Chauveau M, *et al.* 1996. Premier rapport préliminaire des travaux sur le site de 'Ayn Manawir (oasis de Kharga). *Bulletin de l'Institut Français d'Archéologie Orientale* **96**: 385–451.